

# Phase structure, band gap and microwave dielectric properties of $\text{Ba}_8\text{Ti}_3\text{Nb}_{4-x}\text{Sb}_x\text{O}_{24}$ ceramics

Liang Fang\*, Congxue Su, Zhenhai Wei, Huanfu Zhou, Hui Zhang

State Key Laboratory Breeding Base of Nonferrous Metals and Specific Materials Processing, Key laboratory of Nonferrous Materials and New Processing Technology, Ministry of Education, Guilin University of Technology, Guilin 541004, China

Received 4 June 2012; received in revised form 21 June 2012; accepted 21 June 2012

Available online 29 June 2012

## Abstract

High dielectric constant and low loss ceramics in the  $\text{Ba}_8\text{Ti}_3\text{Nb}_{4-x}\text{Sb}_x\text{O}_{24}$  ( $x=0-2$ ) system were prepared by conventional solid-state ceramic route. As  $x$  increased from 0 to 1.5, a single phase with hexagonal 8H perovskite structure was formed and the band gap values increased from 3.38 to 3.47 eV. However, the  $\text{Sb}_2\text{O}_3$  secondary phase was detected as the  $x$  reached 2. The optimum sintering temperature was reduced from 1460 to 1380 °C, the quality factors ( $Q \times f$ ) were effectively enhanced from 22,900 to 38,000 GHz and  $\tau_f$  was significantly lowered from 110 ppm/°C to 2 ppm/°C, whereas the dielectric constant decreased from 49 to 35. A good combined microwave dielectric properties with  $\epsilon_r=37.5$ ,  $Q \times f=38,000$  GHz,  $\tau_f=15$  ppm/°C were obtained for  $x=1.5$ . © 2012 Elsevier Ltd and Techna Group S.r.l. All rights reserved.

**Keywords:** A. Sintering; C. Dielectric properties; D. Perovskites; D. Niobates

## 1. Introduction

The recent advances in the telecommunication systems have attracted considerable attention towards the microwave ceramic dielectric resonators. Dielectric resonators (DRs) are extensively used in microwave devices such as filters, oscillators, and DR antennas. To meet the requirements of DRs applications, the materials should have high dielectric constant  $\epsilon_r$ , relatively high quality factor  $Q$ , ( $Q \times f$  value is usually used as a figure of merit) and near zero temperature coefficient of resonant frequency ( $\tau_f$ ). Among current commercial microwave dielectric materials, extensive attention has been focused on perovskite type structure materials, especially the tantalite and niobate perovskites due to the high polarizability of  $\text{Ta}^{5+}$  and  $\text{Nb}^{5+}$  [1].

Recently, there has been a growing interest in the dielectric properties of hexagonal perovskites [2–4], and many researches have been focused on B-site cation deficient hexagonal perovskites with the formula  $\text{A}_n\text{B}_{n-1}\text{O}_{3n}$  ( $n=4-8$ ) which are based on cubic close packing (c) and hexagonal close packing (h) of the  $\text{AO}_3$  layers. Trolliard

et al. [5], classified  $\text{A}_n\text{B}_{n-1}\text{O}_{3n}$  hexagonal perovskites into shifted and twinned structures, depending on the stacking sequences of their  $\text{AO}_3$  layers. Shifted perovskites can be represented by a packing sequence (hhcc...c) while twinned perovskites can be represented by the packing sequence (hcc...c) which is favored by high values of  $n$  (number of octahedra layers within a perovskite blocks) and  $t$  (Goldschmidt tolerance factor). The microwave dielectric properties of some B-site deficient twinned perovskites such as  $\text{Ba}_8\text{Ti}_3\text{Nb}_4\text{O}_{24}$ ,  $\text{Ba}_8\text{MTa}_6\text{O}_{24}$  ( $\text{M}=\text{Mg}, \text{Zn}, \text{Ni}, \text{Co}, \text{Cu}$ ) and  $\text{Ba}_8\text{Ga}_{4-x}\text{Ta}_{4+0.6x}\text{O}_{24}$  were reported successively [6–12]. These materials exhibit high  $\epsilon_r$  in the range of 27–49, high quality factors  $Q \times f$  up to 90,000 GHz, but a relatively large  $\tau_f$  over 30 ppm/°C. Among them,  $\text{Ba}_8\text{Ti}_3\text{Nb}_4\text{O}_{24}$  possesses an encouraging high  $\epsilon_r$  of 49 and a high  $Q \times f$  (23,500 GHz), but its relatively high  $\tau_f$  (~120 ppm/°C) precludes its use as DRs device [6,7]. Recently, Yokoi et al. [13] reported the substitution of Ta for Nb in  $\text{Ba}_8\text{Ti}_3\text{Nb}_{4-x}\text{Ta}_x\text{O}_{24}$  solid solutions could reduce the  $\tau_f$  from 125 to 76 ppm/°C and increase  $Q \times f$  value. Therefore, the substitution of the other elements in this system is necessary in order to further adjust the  $\tau_f$  values. The ionic radius of  $\text{Sb}^{5+}$  (0.6 Å) is very similar to that of  $\text{Nb}^{5+}$  (0.64 Å) [14]. Moreover, Sb substitution for

\*Corresponding author. Fax: +86 773 5896436.

E-mail address: [fangliangskl@yahoo.com.cn](mailto:fangliangskl@yahoo.com.cn) (L. Fang).

Nb has been reported to effectively reduce  $\tau_f$  in the  $\text{Ba}_8\text{M}(\text{Nb}_{6-x}\text{Sb}_x)\text{O}_{24}$  ( $\text{M}=\text{Zn}, \text{Mg}$ ) and  $\text{Mg}_4(\text{Nb}_{2-x}\text{Sb}_x)\text{O}_9$  ( $x=0-1$ ) ceramics [1,15,16]. In this paper, the  $\text{Ba}_8\text{Ti}_3\text{Nb}_{4-x}\text{Sb}_x\text{O}_{24}$  solid solutions were prepared, and the influences of the Sb substitution for Nb on the structures, sintering behaviors and the microwave dielectric properties of  $\text{Ba}_8\text{Ti}_3\text{Nb}_{4-x}\text{Sb}_x\text{O}_{24}$  ( $x=0-2$ ) ceramics have also been investigated.

## 2. Experimental procedure

$\text{Ba}_8\text{Ti}_3\text{Nb}_{4-x}\text{Sb}_x\text{O}_{24}$  ( $x=0-2$ ) ceramics were prepared by conventional mixed oxide route by using high-purity powders of  $\text{BaCO}_3$  (99.9%),  $\text{TiO}_2$  (99.99%),  $\text{Nb}_2\text{O}_5$  (99.99%), and  $\text{Sb}_2\text{O}_3$  (99%). Stoichiometric proportions of the above raw materials were milled in alcohol using zirconia balls for 4 h. The mixtures were dried and subsequently calcined at 1350 °C for 12 h. The calcined powders were milled for 6 h and the slurry was dried in agate mortar and ground well. Polyvinyl alcohol (5 wt%) was added to the powders as binder, again ground well and dried. The powders were then pressed into cylindrical disks with 12 mm diameter and 7 mm height under a pressure of 200 MPa. The samples were fired at 550 °C for 4 h to remove the organic binder and then sintered in air on a Pt foil at 1360–1480 °C for 6 h. The sintered samples were pulverized in agate mortar and pestle and ground into powder for XRD. An X-ray diffractometer ( $\text{CuK}\alpha_1$ , 1.54059 Å, Model XPert PRO, PANalytical, Almelo, the Netherlands) was used for phase analysis. In order to investigate the band gap energy of  $\text{Ba}_8\text{Ti}_3\text{Nb}_{4-x}\text{Sb}_x\text{O}_{24}$  ( $x=0-1.5$ ) solid solutions, the room temperature UV–vis absorption spectra of the  $\text{Ba}_8\text{Ti}_3\text{Nb}_{4-x}\text{Sb}_x\text{O}_{24}$  powders were measured in the range of 200–800 nm using UV–vis spectrophotometer (UV-3600, Shimadzu) with  $\text{BaSO}_4$  coated integration sphere. The apparent densities of the sintered samples were measured by the Archimedes method. The theoretical densities of the samples were calculated using the least-square method. The surface microstructures of the samples were examined using a field emission scanning electron microscope (FE-SEM, Model S4800, Hitachi, Japan). The microwave dielectric properties were obtained using a network analyzer (Model N5230A, Agilent Co., Palo Alto, Canada) and a temperature chamber (Delta 9039, Delta Design, San Diego, CA). The temperature coefficient of resonant frequency ( $\tau_f$ ) was measured in the temperature range from 25 °C to 85 °C. The  $\tau_f$  value was calculated as follows:

$$\tau_f = \frac{f_{85} - f_{25}}{60 \times f_{25}} \quad (1)$$

where  $f_{85}$  and  $f_{25}$  are the resonant frequencies at 85 °C and 25 °C, respectively.

## 3. Results and discussion

The X-ray diffraction (XRD) patterns of  $\text{Ba}_8\text{Ti}_3\text{Nb}_{4-x}\text{Sb}_x\text{O}_{24}$  ( $x=0-2$ ) ceramics sintered at 1420 °C for 6 h are given in Fig. 1. All the peaks can be indexed according to

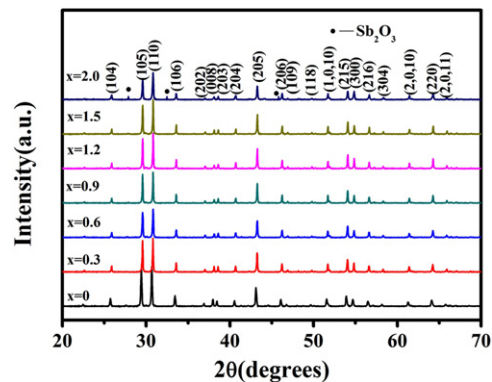


Fig. 1. X-ray diffraction pattern of  $\text{Ba}_8\text{Ti}_3\text{Nb}_{4-x}\text{Sb}_x\text{O}_{24}$  ( $x=0-2$ ) ceramics sintered at 1420 °C for 6 h.

Table 1

The unit cell parameters of  $\text{Ba}_8\text{Ti}_3\text{Nb}_{4-x}\text{Sb}_x\text{O}_{24}$  ( $x=0-2$ ) ceramics.

$x$	$a$ (Å)	$c$ (Å)	$c/a$	$V_m$ (Å <sup>3</sup> )
0	5.7941	18.8674	3.2563	548.55
0.3	5.7929	18.8648	3.2565	548.16
0.6	5.7918	18.8630	3.2568	547.99
0.9	5.7905	18.8593	3.2570	547.63
1.2	5.7892	18.8559	3.2571	547.28
1.5	5.7871	18.8503	3.2573	546.72
2.0	5.7869	18.8472	3.2569	546.60

$\text{Ba}_8\text{Ti}_3\text{Nb}_4\text{O}_{24}$  (PDF files 00-054-1170), which has a hexagonal perovskite structure (space group  $\text{P6}_3/\text{mmc}$ ) based on  $8\text{H}(\text{hccc})_2$  closed-packed arrangement of  $\text{BaO}_3$  layers [5]. The fully indexed XRD patterns confirmed that  $\text{Ba}_8\text{Ti}_3\text{Nb}_{4-x}\text{Sb}_x\text{O}_{24}$  ceramics are single phase as  $x \leq 1.5$ , and the presence of  $\text{Sb}_2\text{O}_3$  phase was detected at  $x=2$ . With increase in  $x$  from 0 to 1.5, diffraction peaks of the samples were slightly shifted to higher angles, which was due to the difference in the ionic radii between the  $\text{Sb}^{5+}$  and  $\text{Nb}^{5+}$  [14]. The lattice parameters of the samples were refined by least squares method and are shown in Table 1. It is obvious that the lattice constants  $a$ ,  $c$  and  $V$  decrease with increasing substitution of Sb content, which is mainly attributed to smaller ionic radius of  $\text{Sb}^{5+}$  than that of  $\text{Nb}^{5+}$ .

The room temperature UV–vis absorption spectra are shown in Fig. 2, the ultraviolet absorption edge of  $\text{Ba}_8\text{Ti}_3\text{Nb}_{4-x}\text{Sb}_x\text{O}_{24}$  ( $x=0-1.5$ ) has a small blue shift with increasing concentration of Sb. The energy gap of the samples can be calculated as follows [17]:

$$(\alpha h\nu)^{1/n} = A(h\nu - E_g) \quad (2)$$

where  $A$  is absorption constant,  $h\nu$  is the photon energy,  $E_g$  is the energy gap and  $n$  depends on the nature of transition. In addition, absorption coefficient  $\alpha$  is proportional to the quantity  $F(R_\infty)$  and thus  $\alpha$  can be substituted with  $F(R_\infty)$ . The reflectance spectra are according to the Kubelka–Munk theory. Based on the best linear fit in the lower absorption region [18,19],  $n=1/2$  is used for these samples.

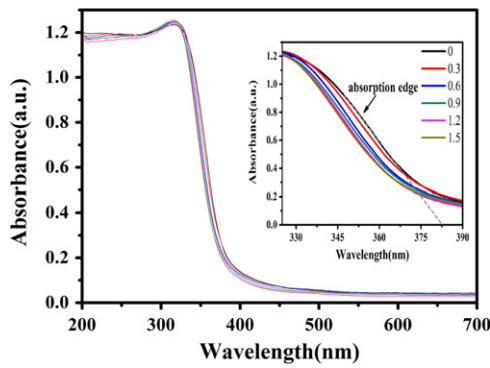


Fig. 2. The room temperature UV–vis absorption spectra of  $\text{Ba}_8\text{Ti}_3\text{Nb}_{4-x}\text{Sb}_x\text{O}_{24}$  ( $x=0-1.5$ ).

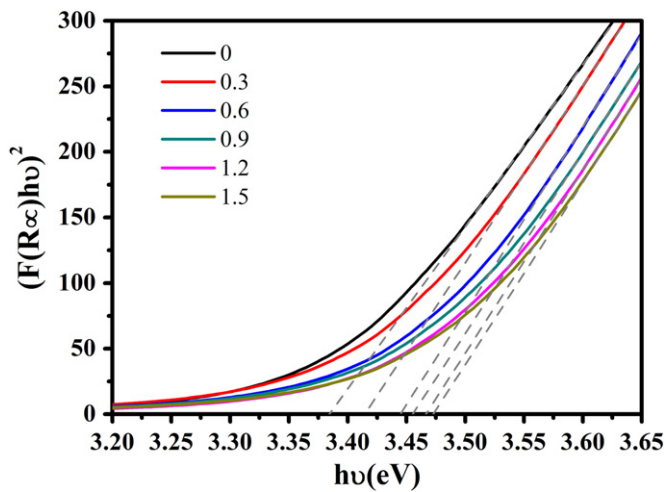


Fig. 3.  $h\nu-(F(R_\infty)/h\nu)^2$  curve of the samples.

The graph between  $(F(R_\infty)/h\nu)^2$  and  $h\nu$  is shown in Fig. 3. It can be observed that the band gap energies increase from 3.38 eV for  $x=0$  to 3.47 eV for  $x=1.5$ . The band gap of  $\text{Ba}_8\text{Ti}_3\text{Nb}_4\text{O}_{24}$  is very close to the previous report (3.4 eV) obtained by impedance spectroscopy measurements [7]. In the microwave frequency, the dielectric loss is proportional to the conductivity, which is decreased as the band gap increased, then the increase of band gap might reduce the intrinsic dielectric loss and hence the  $Q \times f$  values increase.

Fig. 4 presents the apparent densities of the  $\text{Ba}_8\text{Ti}_3\text{Nb}_{4-x}\text{Sb}_x\text{O}_{24}$  ( $x=0-2$ ) ceramics as a function of sintering temperature. The apparent densities of ceramics increase with increasing sintering temperature, reach a maximum value and then decrease. The maximum values of density for  $\text{Ba}_8\text{Ti}_3\text{Nb}_{4-x}\text{Sb}_x\text{O}_{24}$  ( $x=0-2$ ) ceramics are more than 95% of theoretical density. The optimum sintering temperature of  $\text{Ba}_8\text{Ti}_3\text{Nb}_{4-x}\text{Sb}_x\text{O}_{24}$  ceramics was slightly reduced from 1460 to 1380 °C with increase in  $x$  value from 0 to 2. Fig. 5(a–d) shows the FE-SEM micrographs of the surfaces of samples with  $x=1.5$  sintered at different temperatures for 6 h. A porous microstructure and small grains below 15  $\mu\text{m}$  were observed in the specimen sintered at 1360 °C. The increase of the sintering temperature

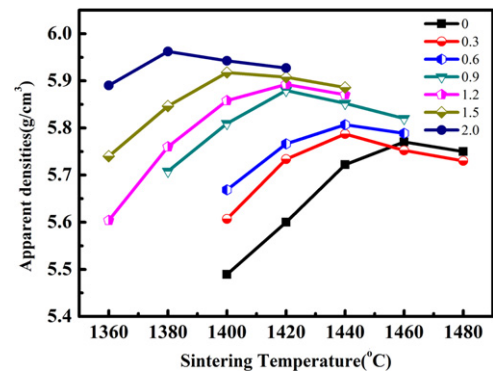


Fig. 4. The variations of apparent density of  $\text{Ba}_8\text{Ti}_3\text{Nb}_{4-x}\text{Sb}_x\text{O}_{24}$  ceramics with different sintering temperatures.

promoted grain growth, and a relatively dense microstructure with grains size in the range from 15 to 20  $\mu\text{m}$  in length was achieved for the specimen sintered at 1380 °C. Denser microstructure without pores and a relatively uniform plate-like grains with size in the range of 25–40  $\mu\text{m}$  has been achieved at 1400 °C, and exaggerated grain growth with large grains ( $> 40 \mu\text{m}$ ) was observed in the ceramic sintered at 1440 °C due to over-sintering.

Upon sintering at the optimized temperature, the ceramics can have excellent microwave dielectric properties. The variations in the dielectric constants and quality factors of the ceramics as a function of compositions  $x$  are shown in Fig. 6. The dielectric constant linearly decreased from 49 to 35 as  $x$  increased from 0 to 2. In general,  $\epsilon_r$  can be well interpreted by the sum of ionic polarizabilities of individual ions ( $\alpha_D^T$ ) and per molar volume ( $V_m$ ) according to Clausius–Mossotti equation:

$$\epsilon_r = \frac{1 + 2b\alpha_D^T/V_m}{1 - b\alpha_D^T/V_m} \quad (3)$$

where  $b=4\pi/3$ . The decreasing dielectric constant was mainly due to the decreasing value of  $\alpha_D^T/V_m$  from 0.192 for  $x=0$  to 0.182 for  $x=2$  since the ionic dielectric polarizability ( $\alpha_D$ ) ( $1.18 \pm 0.49 \text{ \AA}^3$ ) of  $\text{Sb}^{5+}$  ions [20] is lower than that of  $\text{Nb}^{5+}$  ions [21]. The quality factor  $Q \times f$  values increased gradually from 22,900 to 38,000 GHz as  $x$  increased to 1.5, and then decreased at  $x=2$ . Ogawa et al. [16] suggested that the Sb substitution for Nb enhances the covalency of Sb–O bond and hence the  $Q \times f$  values increase and  $\epsilon_r$  decreases. The lower quality factor for the samples with  $x=2$  may be attributed to the formation of secondary phases as mentioned above.

The temperature coefficients of resonant frequency ( $\tau_f$ ) was adjusted from 110 to 2 with increasing Sb content from 0 to 2 (as shown in Fig. 7), which is also similar to those of  $\text{Ba}_8\text{M}(\text{Nb}_{6-x}\text{Sb}_x)\text{O}_{24}$  ( $\text{M}=\text{Zn}, \text{Mg}$ ) ( $x=0-2.4$ ) [1,15] and  $\text{Ba}_3\text{M}\text{Nb}_{2-x}\text{Sb}_x\text{O}_9$  ( $\text{M}=\text{Mg}, \text{Ni}, \text{Zn}$ ) [22]. Two mechanisms [23–25] determine the tunability of  $\tau_f$  in perovskites and related compounds: one is dilution of the average ionic polarizability and the other is the onset of octahedral tilt transitions induced by decreasing tolerance factor. Tolerance factors ( $t$ ) are greater than 1 in  $\text{Ba}_8\text{Ti}_3\text{Nb}_{4-x}\text{Sb}_x\text{O}_{24}$  solid solutions, which rules out

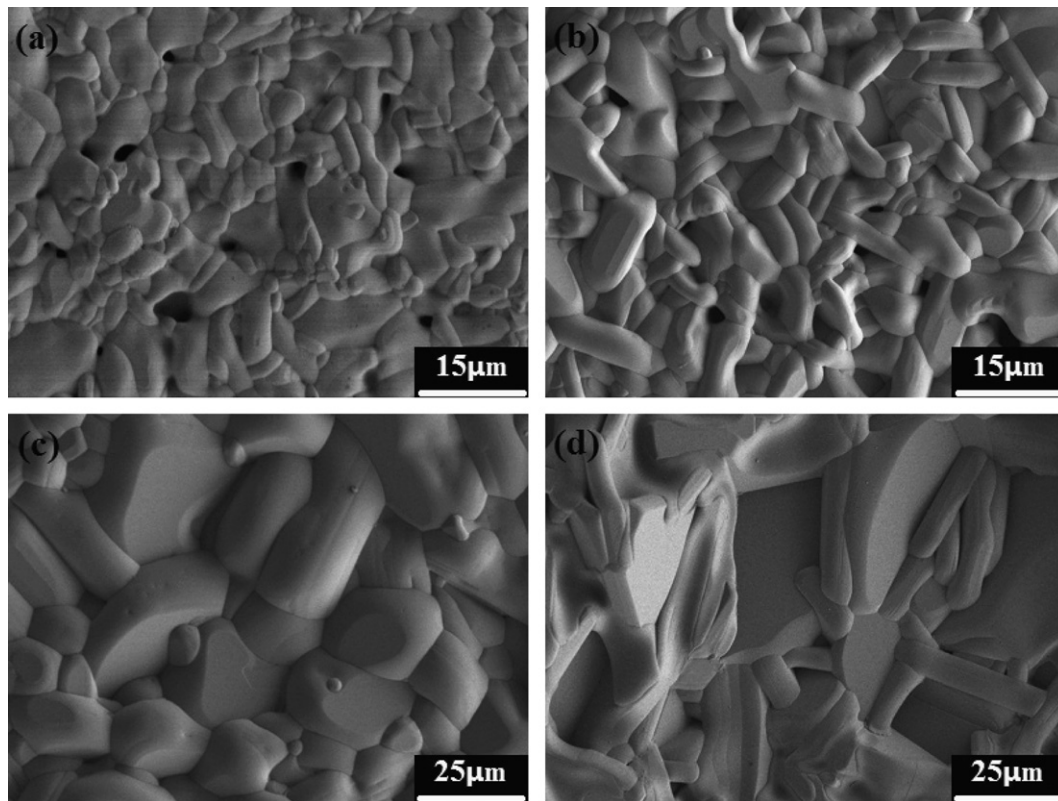


Fig. 5. FE-SEM images of the surfaces of  $\text{Ba}_8\text{Ti}_3\text{Nb}_{2.5}\text{Sb}_{1.5}\text{O}_{24}$  ceramics sintered at different temperatures: (a) 1360 °C; (b) 1380 °C; (c) 1400 °C; (d) 1440 °C.

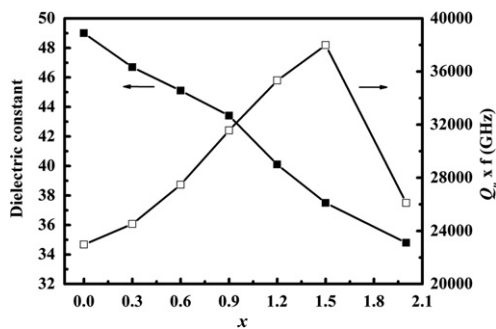


Fig. 6. The variations of  $\epsilon_r$  and  $Q \times f$  of  $\text{Ba}_8\text{Ti}_3\text{Nb}_{4-x}\text{Sb}_x\text{O}_{24}$  ceramics with  $x$ .

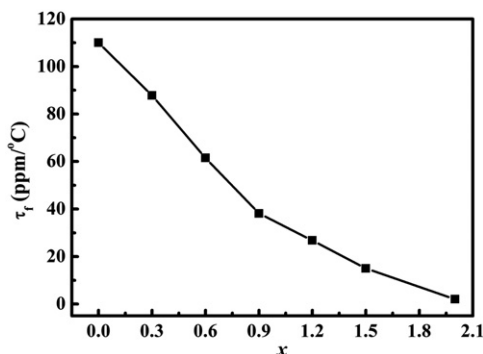


Fig. 7. The variations of  $\tau_f$  of  $\text{Ba}_8\text{Ti}_3\text{Nb}_{4-x}\text{Sb}_x\text{O}_{24}$  ceramics with  $x$ .

the possibility for an octahedral tilting transition. So the primary mechanism of  $\tau_f$  tunability is attributed to the reduction of the average ionic polarizability. Zhou et al. [26,27] reported a linear relationship between  $\tau_c$  and  $\epsilon_r$  and therefore also between  $\tau_f$  and  $\epsilon_r$ . In this work, a similar linear trend (shown in Figs. 6 and 7) is apparent for  $\text{Ba}_8\text{Ti}_3\text{Nb}_{4-x}\text{Sb}_x\text{O}_{24}$  samples, also implying that  $\tau_f$  decreases as the  $\epsilon_r$  diminishes.

#### 4. Conclusion

$\text{Ba}_8\text{Ti}_3\text{Nb}_{4-x}\text{Sb}_x\text{O}_{24}$  ( $x=0-2$ ) ceramics were prepared through a mixed oxide solid state sintering route at 1360–1480 °C. A single phase with hexagonal 8H perovskite structure was formed in the range  $0 \leq x \leq 1.5$ , while secondary phase appeared at  $x=2$ . The optimized sintering temperature was reduced from 1460 to 1380 °C. The substitution of Sb for Nb could effectively improve the quality factor and reduce  $\tau_f$  values. As the  $x$  values increased to 1.5, the band gap values increased from 3.38 to 3.47 eV, quality factor  $Q \times f$  effectively enhanced from 22,900 to 38,000 GHz. In the range of  $x=0$  to 2,  $\tau_f$  value improved from 110 to 2 ppm/°C, whereas  $\epsilon_r$  decreased from 49 to 35.

#### Acknowledgment

This work was supported by Natural Science Foundation of China (nos. 50962004, 21061004 and 51102058),



Project of Department of Science and Technology of Guangxi (nos. 10-046-01, 11-031-03 and 11107006-42), and Program to Sponsor Teams for Innovation in the Construction of Talent Highlands in Guangxi Institutions of Higher Learning.

## References

- [1] M.K. Suresh, J. Annamma, J.K. Thomas, P.R.S. Wariar, S. Solomon, Structural, spectroscopic and dielectric investigations on  $\text{Ba}_8\text{Zn}(\text{Nb}_{6-x}\text{Sb}_x)\text{O}_{24}$  microwave ceramics, *Materials Research Bulletin* 45 (2010) 1389–1395.
- [2] D.J. Chu, L. Fang, H.F. Zhou, X.L. Chen, Z. Yang, Effects of  $\text{BaCu}(\text{B}_2\text{O}_5)$  addition on phase transition, sintering temperature and microwave properties of  $\text{Ba}_4\text{LiTa}_3\text{O}_{12}$  ceramics, *Journal of Alloys and Compounds* 509 (2011) 1931–1935.
- [3] H. Zhang, Y.M. Wu, S.S. Meng, L. Fang, Crystal structure and microwave dielectric properties of a new  $\text{A}_4\text{B}_3\text{O}_{12}$ -type cation-deficient perovskite  $\text{Ba}_3\text{LaTa}_3\text{O}_{12}$ , *Journal of Alloys and Compounds* 460 (2008) 460–463.
- [4] L. Fang, D.J. Chu, C.C. Li, H.F. Zhou, Z. Y, Effects of  $\text{BaCu}(\text{B}_2\text{O}_5)$  addition on phase transition, sintering temperature, and microwave properties of  $\text{Ba}_4\text{LiNb}_3\text{O}_{12}$  ceramics, *Journal of the American Ceramic Society* 94 (2011) 524–528.
- [5] G. Trolliard, N. Teneze, Ph. Boullay, D. Mercurio, TEM study of cation-deficient-perovskite related  $\text{A}_n\text{B}_{n-1}\text{O}_{3n}$  compounds: the twin-shift option, *Journal of Solid State Chemistry* 177 (2004) 1188–1196.
- [6] L. Fang, L. Chen, H. Zhang, X.K. Hong, C.L. Diao, H.X. Liu, Microwave dielectric properties of  $\text{Ba}_{5+n}\text{Ti}_n\text{Nb}_4\text{O}_{15+3n}$  ceramics, *Journal of Materials Science: Materials in Electronics* 16 (2005) 149–151.
- [7] R. Rawal, A. Feteira, A.A. Flores, N.C. Hyatt, A.R. West, D.C. Sinclair, Dielectric properties of the twinned 8H-hexagonal perovskite  $\text{Ba}_8\text{Nb}_4\text{Ti}_3\text{O}_{24}$ , *Journal of the American Ceramic Society* 89 (2006) 336–339.
- [8] S.M. Moussa, J.B. Claridge, M.J. Rosseinsky, S. Clarke, R.M. Ibberson, T. Price, D.M. Iddles, D.C. Sinclair,  $\text{Ba}_8\text{ZnTa}_6\text{O}_{24}$ : a high-Q microwave dielectric from a potentially diverse homologous series, *Applied Physics Letters* 82 (2003) 4537–4539.
- [9] M. Thirumal, P.K. Davies,  $\text{Ba}_8\text{ZnTa}_6\text{O}_{24}$ : a new high Q dielectric perovskite, *Journal of the American Ceramic Society* 88 (2005) 2126–2128.
- [10] S. Kawaguchi, H. Ogawa, A. Kan, S. Ishihara, Microwave dielectric properties of  $\text{Ba}_8\text{Ta}_6(\text{Ni}_{1-x}\text{M}_x)\text{O}_{24}$  ( $\text{M}=\text{Zn}$  and  $\text{Mg}$ ) ceramics, *Journal of the European Ceramic Society* 26 (2006) 2045–2049.
- [11] A. Kan, H. Ogawa, A. Yokoi, H. Ohsato, Microwave dielectric properties of perovskites-like structured  $\text{Ba}_8\text{Ta}_6(\text{Ni}_{1-x}\text{M}_x)\text{O}_{24}$  ( $\text{M}=\text{Co}$ ,  $\text{Cu}$ , and  $\text{Zn}$ ) solid solutions, *Japanese Journal of Applied Physics* 45 (2006) 7494–7498.
- [12] J. Cao, X.J. Kuang, M. Allix, C. Dickinson, J.B. Claridge, M.J. Rosseinsky, D.M. Iddles, Q. Su, New 8-layer twinned hexagonal perovskite microwave dielectric ceramics  $\text{Ba}_8\text{Ga}_{4-x}\text{Ta}_{4+0.6x}\text{O}_{24}$ , *Chemistry of Materials* 23 (2011) 5058–5067.
- [13] A. Yokoi, H. Ogawa, A. Kan, Microwave dielectric properties of  $\text{BaO}-\text{Ta}_2\text{O}_5-\text{TiO}_2$  system, *Journal of the European Ceramic Society* 26 (2006) 2069–2074.
- [14] R.D. Shannon, Revised effective ionic radii in halides and chalcogenides, *Acta Crystallographica Section A: Crystal Physics, Diffraction, Theoretical and General Crystallography* 32 (1976) 751–767.
- [15] M.K. Suresh, J. Annamma, J.K. Thomas, P.R.S. Wariar, S. Solomon, Structural analysis and properties of thermally stable  $\text{Ba}_8\text{Mg}(\text{Nb}_{6-x}\text{Sb}_x)\text{O}_{24}$  microwave ceramics, *Journal of Alloys and Compounds* 509 (2011) 2401–2406.
- [16] H. Ogawa, H. Taketani, A. Kan, A. Fujita, G. Zouganelis, Evaluation of electronic state of  $\text{Mg}_4(\text{Nb}_{2-x}\text{Sb}_x)\text{O}_9$  microwave dielectric ceramics by first principle calculation method, *Journal of the European Ceramic Society* 25 (2005) 2859–2863.
- [17] E.A. Davis, N.F. Mott, Conduction in non-crystalline systems V. Conductivity, optical absorption and photoconductivity in amorphous semiconductors, *Philosophical Magazine* 22 (1970) 903–922.
- [18] A.A. Hossein, C.A. Hogarth, J. Beynon, Optical absorption in  $\text{CeO}_2-\text{V}_2\text{O}_5$  evaporated thin films, *Journal of Materials Science Letters* 13 (1994) 1144–1145.
- [19] G.A. Khan, C.A. Hogarth, Optical absorption spectra of evaporated  $\text{V}_2\text{O}_5$  and co-evaporated  $\text{V}_2\text{O}_5/\text{B}_2\text{O}_3$  thin films, *Journal of Materials Science Letters* 26 (1991) 412–416.
- [20] S.C. Tidrow, A. Tauber, W.D. Wilber, R.D. Finnegan, D.W. Eckart, W.C. Drach, Dielectric properties of perovskite antimonates, *IEEE Transactions on Applied Superconductivity* 7 (2) (1997) 1769–1771.
- [21] R.D. Shannon, Dielectric polarizabilities of ions in oxides and fluorides, *Journal of Applied Physics* 73 (1993) 348–366.
- [22] M.W. Lufaso, E. Hopkins, S.M. Bell, A. Llobet, Crystal chemistry and microwave dielectric properties of  $\text{Ba}_3\text{MnNb}_{2-x}\text{Sb}_x\text{O}_9$  ( $\text{M}=\text{Mg}$ ,  $\text{Ni}$ ,  $\text{Zn}$ ), *Chemistry of Materials* 17 (2005) 4250–4255.
- [23] P.L. Wise, I.M. Reaney, W.E. Lee, D.M. Iddles, D.S. Cannell, T.J. Price, Tunability of  $\tau_f$  in perovskites and related compounds, *Journal of Materials Research* 17 (2002) 2033–2040.
- [24] I.M. Reaney, P.L. Wise, R. Ubic, J. Breeze, N.M. Alford, D. Iddles, D. Cannell, T.J. Price, On the temperature coefficient of resonant frequency in microwave dielectric, *Philosophical Magazine A* 81 (2001) 501–510.
- [25] P.L. Wise, I.M. Reaney, W.E. Lee, T.J. Price, D.M. Iddles, D.S. Cannell, Structure-microwave property relations in  $(\text{Sr}_x\text{Ca}_{1-x})_{n+1}\text{TiO}_{3n+1}$ , *Journal of the European Ceramic Society* 21 (2001) 1723–1726.
- [26] D. Zhou, C.A. Randall, H. Wang, L.X. Pang, X. Yao, Microwave dielectric properties trends in a solid solution  $(\text{Bi}_{1-x}\text{Ln}_x)_2\text{Mo}_2\text{O}_9$  ( $\text{Ln}=\text{La}$ ,  $\text{Nd}$ ,  $0.0 \leq x \leq 0.2$ ) system, *Journal of the American Ceramic Society* 92 (2009) 2931–2936.
- [27] L.X. Pang, H. Wang, D. Zhou, X. Yao, A new temperature stable microwave dielectric with low-firing temperature in  $\text{Bi}_2\text{MoO}_6-\text{TiO}_2$  system, *Journal of Alloys and Compounds* 493 (2010) 626–629.